

Searching for $H \rightarrow \gamma\gamma$ in weak boson fusion at the LHC

D. Rainwater and D. Zeppenfeld

Department of Physics, University of Wisconsin, Madison, WI 53706

Abstract

Weak boson fusion is a copious source of intermediate mass Higgs bosons at the LHC, with a rate $\sigma B(H \rightarrow \gamma\gamma)$ of up to 9 fb. The additional very energetic forward jets in these events provide for a unique signature. A parton level analysis of the dominant backgrounds demonstrates that this channel allows the observation of $H \rightarrow \gamma\gamma$ in a low background environment, with modest luminosity.

The search for the Higgs boson and, hence, for the source of electroweak symmetry breaking and fermion mass generation, remains one of the premier tasks of present and future high energy physics experiments. Fits to precision electroweak (EW) data have for some time suggested a relatively low Higgs boson mass, in the 100 GeV range [1] and this is one of the reasons why the search for an intermediate mass Higgs boson is particularly important [2]. Beyond the reach of LEP, for masses in the 100 – 150 GeV range, the $H \rightarrow \gamma\gamma$ decay channel at the CERN LHC is very promising. Consequently, LHC detectors are designed with excellent photon detection capabilities, resulting in a di-photon mass resolution of order 1 GeV for a Higgs boson mass around 120 GeV [3]. Another advantage of the $H \rightarrow \gamma\gamma$ channel, in particular compared to the dominant $H \rightarrow b\bar{b}$ mode, is the lower background from QCD processes.

For this intermediate mass range, most of the literature has focussed on Higgs production via gluon fusion [2], and $t\bar{t}H$ [4] or $WH(ZH)$ [5] associated production. While production via gluon fusion has the largest cross section by about an order of magnitude, there are substantial QCD backgrounds but few handles to distinguish them from the signal. Essentially, only the decay photons' transverse momentum and the sharp resonance in the $\gamma\gamma$ invariant mass distribution can be used.

It is necessary to study other production channels for several reasons. For instance, electroweak symmetry breaking and fermion mass generation may be less intimately connected than in the Standard Model (SM) and the coupling of the lightest Higgs resonance to fermions might be severely suppressed. In this case, neither $gg \rightarrow H$ fusion nor $t\bar{t}H$ associated production would be observed. Once the Higgs boson is observed in both $gg \rightarrow H$ and the weak boson fusion process $qq \rightarrow qqH$, where the Higgs is radiated off virtual W 's or Z 's, the cross section ratio of these modes measures the ratio of the Higgs coupling to the top quark and to W, Z . This value is fixed in the SM, but deviations are expected in more general models, like supersymmetry with its two Higgs doublets [6]. Finally, as we shall demonstrate, the weak boson fusion channel may yield a quicker discovery, requiring only 10-20 fb⁻¹, which compares favorably to the integrated luminosity required for discovery in the $gg \rightarrow H \rightarrow \gamma\gamma$ channel [3].

Our analysis is a parton-level Monte Carlo study, using full tree-level matrix elements of the

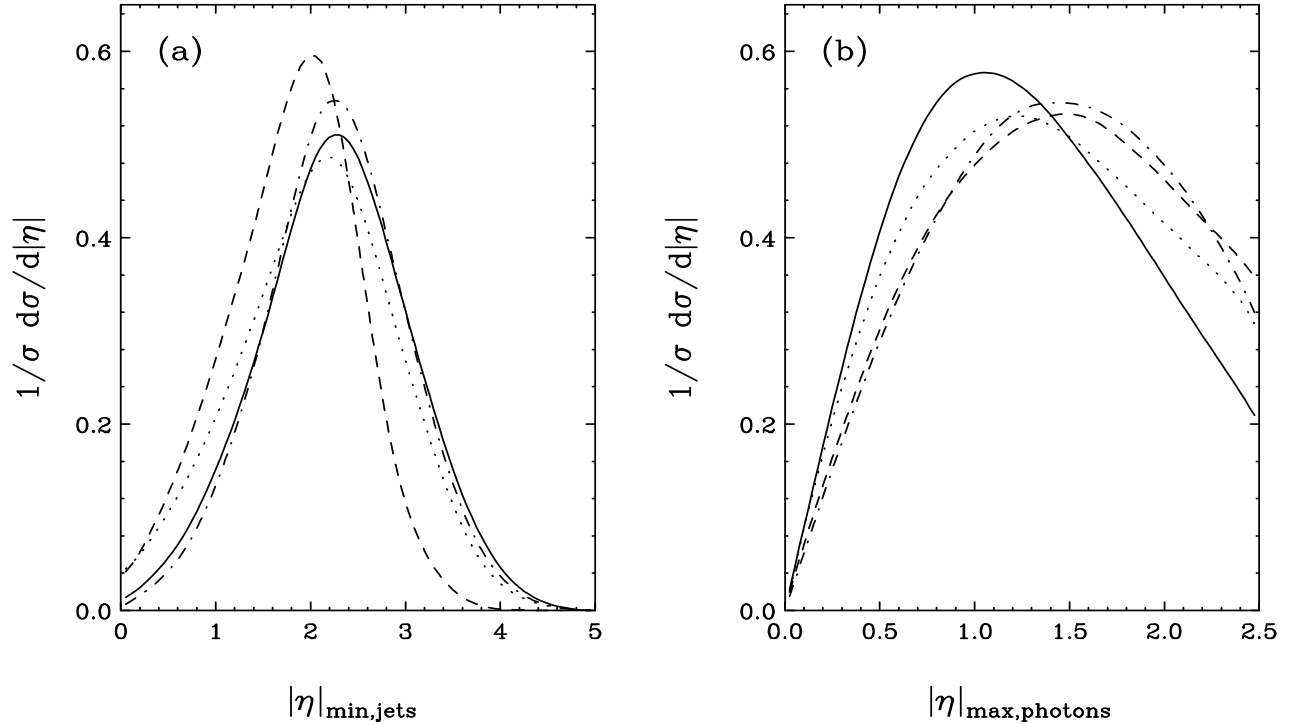


FIG. 1. Normalized pseudo-rapidity distributions of (a) the most central tagging jet and (b) the photon closest to the beam axis in $jj\gamma\gamma$ events at the LHC. The generic acceptance cuts of Eq. (1) and the forward jet tagging cuts of Eq. (2) are imposed. Results are shown for the $qq \rightarrow qqH$ signal at $m_H = 120$ GeV (solid line) for the irreducible QCD background (dashed line), the irreducible EW background (dot-dashed line), and for the double parton scattering (DPS) background (dotted line).

weak boson fusion Higgs signal and the various backgrounds. Cross sections for Higgs production at the LHC are well-known [2]. For a Higgs in the intermediate mass range, the weak boson fusion cross section is approximately one order of magnitude smaller than for gluon fusion. Features of the signal are a centrally produced Higgs which tends to yield central photons, and two jets which enter the detector at large rapidity compared to the photons (see Fig. 1). Another characteristic feature of the signal are the semi-hard transverse momentum distributions of the jets and photons which are shown in Figs. 2 and 3. The $p_{T_{max}}$ distributions of the signal peak well above detector thresholds, which allows for higher jet and photon p_T cuts to reduce the background while retaining a large signal acceptance. For the photons, the growth of the median

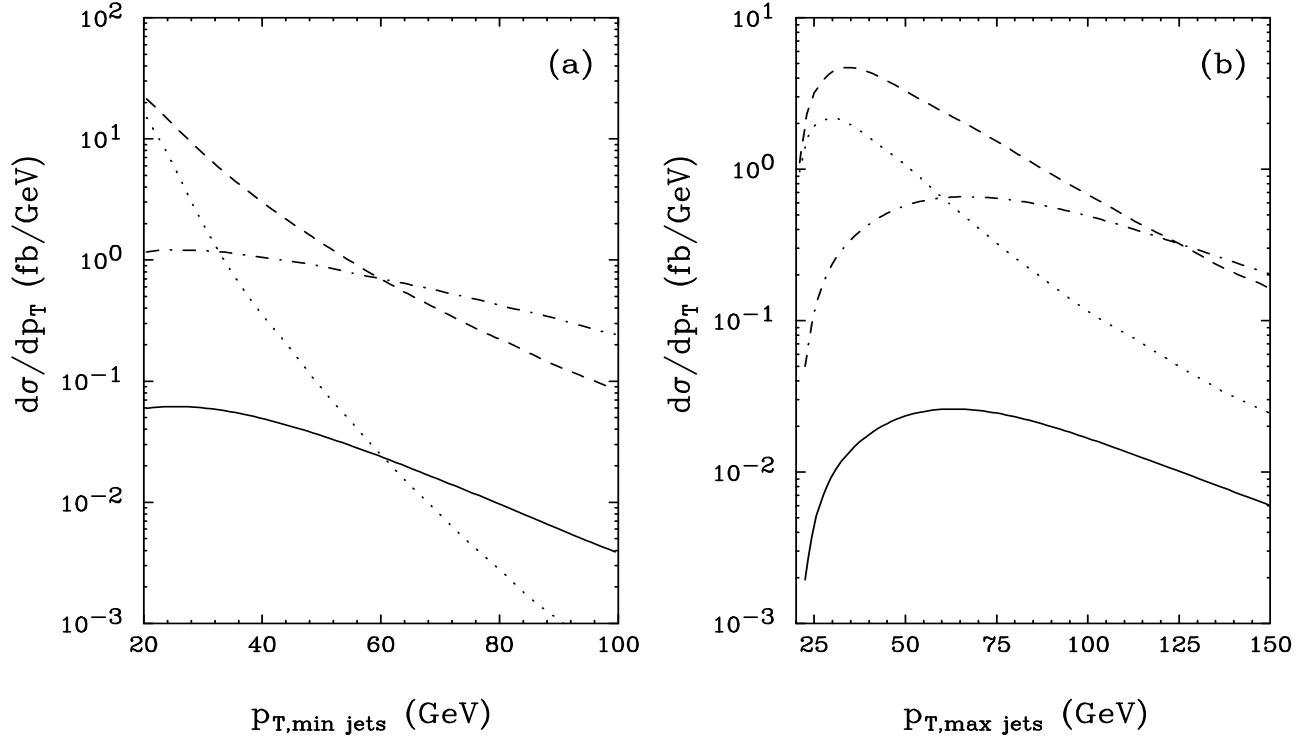


FIG. 2. Transverse momentum distributions of (a) the softer and (b) the harder of the two tagging jets in $jj\gamma\gamma$ events. Generic acceptance cuts (Eq. (1)) and forward jet tagging cuts (Eq. (2)). are imposed. The signal (solid curve) and the backgrounds are labeled as in Fig. 1.

photon p_T with Higgs mass improves the signal acceptance when searching at the upper end of the intermediate mass range.

The signal can be described, at tree level, by two single-Feynman-diagram processes, WW and ZZ fusion where the weak bosons are emitted from the incoming quarks. For the $H \rightarrow \gamma\gamma$ partial decay width it is sufficient to include only the contribution from t and W loops. As for the backgrounds, we use CTEQ4M parton distribution functions [7] and the EW parameters $m_Z = 91.188$ GeV, $m_t = 175.0$ GeV, $\sin^2 \theta_W = 0.2315$, and $G_F = 1.16639 \times 10^{-5}$ GeV $^{-2}$. We choose the factorization scale $\mu_f = \text{minimum } p_T \text{ of the jets}$.

We consider three levels of cuts. The basic acceptance requirement ensures that two photons and two jets are observed in the detector, with very high trigger efficiency [3]:

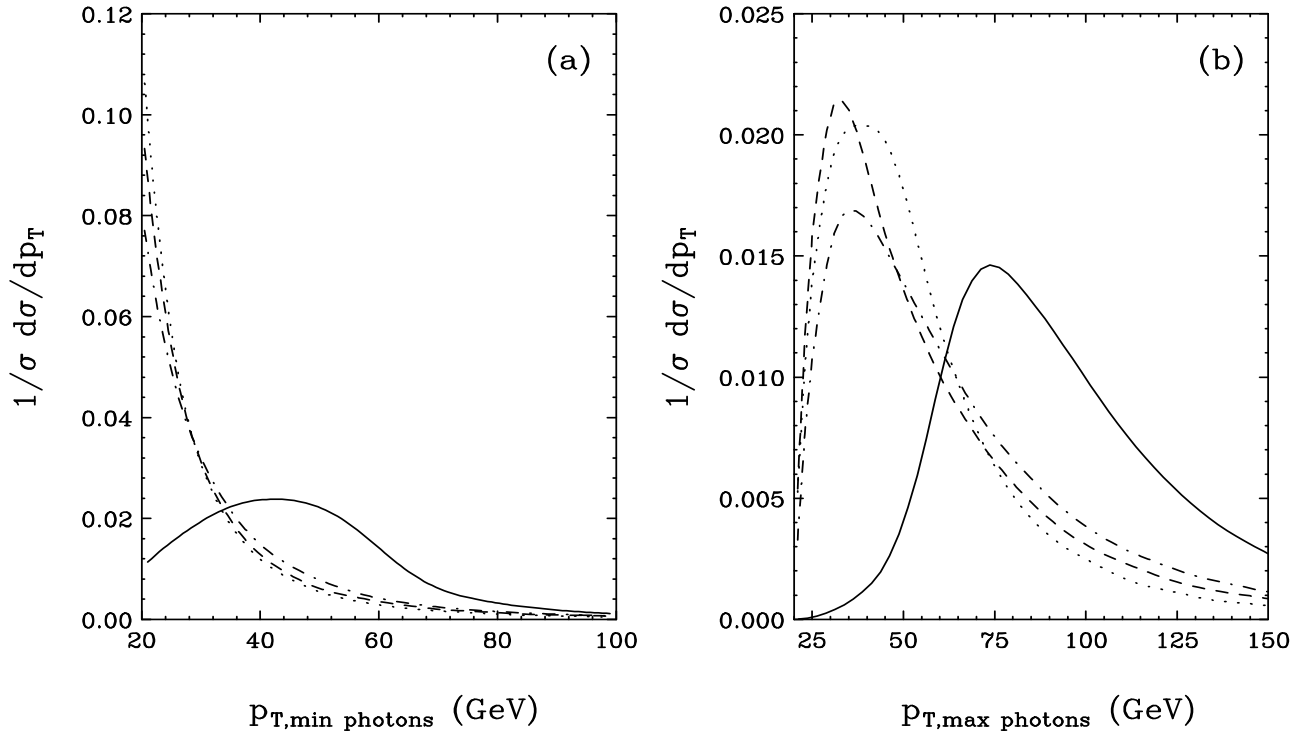


FIG. 3. Transverse momentum distributions of (a) the softer and (b) the harder of the two photons in $jj\gamma\gamma$ events. Generic acceptance cuts (Eq. (1)) and forward jet tagging cuts (Eq. (2)) are imposed. The signal (solid curve) and the backgrounds are labeled as in Fig. 1.

$$\begin{aligned}
p_{T_j} &\geq 20 \text{ GeV} , & p_{T_\gamma} &\geq 20 \text{ GeV} , \\
|\eta_j| &\leq 5.0 , & |\eta_\gamma| &\leq 2.5 , \\
\Delta R_{jj} &\geq 0.7 , & \Delta R_{j\gamma} &\geq 0.7 .
\end{aligned} \tag{1}$$

At the second level, double forward jet tagging is required, with two jets in opposite hemispheres and the photons located between the jets in pseudo-rapidity:

$$\begin{aligned}
\Delta\eta_{tags} = |\eta_{j_1} - \eta_{j_2}| &\geq 4.4 , & \eta_{j_1} \cdot \eta_{j_2} &< 0 , \\
\min\{\eta_{j_1}, \eta_{j_2}\} + 0.7 &\leq \eta_\gamma \leq \max\{\eta_{j_1}, \eta_{j_2}\} - 0.7 .
\end{aligned} \tag{2}$$

This technique to separate weak boson scattering from various backgrounds is well-established [8–10], in particular for heavy Higgs boson searches. For $m_H = 120$ GeV, the cuts of Eqs. (1) and (2) yield cross sections of 5.1 and 2.4 fb, respectively.

Given the features of the signal, we need to consider background processes that can lead to

events with two hard, isolated photons and two forward jets. The prime sources are irreducible QCD and EW $2\gamma + 2\text{jet}$ processes. Double parton scattering (DPS), with pairs of jets and/or photons arising from two independent partonic collisions in one pp interaction, is considered also. We do not consider reducible backgrounds, where e.g. a jet fragmenting into a leading π^0 is misidentified as a photon. Reducible backgrounds were shown to be small compared to irreducible ones in the analysis of the $gg \rightarrow H \rightarrow \gamma\gamma$ signal [3] and we assume the same to hold for the cleaner signal considered here. Matrix elements for the irreducible QCD processes are available in the literature [11], but we are not aware of previous calculations of the irreducible EW background. To generate the matrix elements for it and the DPS codes we use Madgraph [12]. The running of α_s is determined at leading order and we take $\alpha_s(M_Z) = 0.118$ throughout.

The largest background consists of all QCD $2 \rightarrow 2$ processes which contain one or two quark lines, from which the two photons are radiated. Examples are $q\bar{Q} \rightarrow q\bar{Q}\gamma\gamma$ or $qg \rightarrow qg\gamma\gamma$. For this irreducible QCD background, the renormalization scale is chosen as the average p_T of the jets, $\mu_r = \frac{1}{n_{jet}} \sum p_{T_{jet}}$, while the factorization scale is taken as the average p_T of the jets and photons, $\mu_f = \frac{1}{n_{part}} \sum p_{T_{all}}$. A prominent feature of the irreducible QCD background is the steeply falling transverse momentum distributions of both the jets and photons, as given by the dashed lines in Figs. 2 and 3. These distributions are typical for bremsstrahlung processes and allow one to suppress the backgrounds further by harder p_T cuts. Another feature of the irreducible QCD background is the generally higher rapidity of the photons (see Fig. 1): photon bremsstrahlung occurs at small angles with respect to the parent quarks, leading to forward photons once the jets are required to be forward.

The irreducible EW background consists of $qQ \rightarrow qQ$ processes mediated by t -channel Z , γ , or W exchange, with additional radiation of two photons. γ and Z exchange processes have amplitudes which are proportional to the ones of analogous gluon exchange processes, but with smaller couplings. We ignore them because, in all regions of phase space, they constitute only a tiny correction to the irreducible QCD background. We do include all charged current $qQ \rightarrow qQ\gamma\gamma$ (and crossing related) processes, however. W exchange processes can produce central photons by emission from the exchanged W and, therefore, are kinematically similar to

the signal. This signal-like component remains after forward jet tagging cuts, as can readily be seen in the p_T distribution of the jets in Fig. 2. While formally of order α^4 and thus suppressed compared to the order α^3 Higgs signal, the small $H \rightarrow \gamma\gamma$ branching ratio leads to comparable event rates. Because kinematic cuts on the jets cannot reduce this background compared to the signal, it is potentially dangerous. The irreducible EW background is determined with the same choice of factorization scale as the irreducible QCD background.

With jet transverse momenta as low as 20 GeV, double parton scattering (DPS) is a potential source of backgrounds. DPS is the occurrence of two distinct hard scatterings in the collision of a single pair of protons. Following Ref. [13], we calculate the cross section for two distinguishable processes, happening in one pp collision, as

$$\sigma_{DPS} = \frac{\sigma_1 \sigma_2}{\sigma_{eff}} , \quad (3)$$

with the additional constraint that the sum of initial parton energies from one proton be bounded by the beam energy. σ_{eff} parameterizes the transverse size of the proton. It has recently been measured by CDF as $\sigma_{eff} = 14.5$ mb [14]. We assume the same value to hold for LHC energies.

One DPS background arises from simultaneous $\gamma\gamma j$ and jj events, where the jet in the $\gamma\gamma j$ hard scattering is observed as a tagging jet, together with one of the two jets in the dijet process. In order to avoid a three-jet signature, one might want to require the second jet of the dijet process to fall outside the acceptance region of Eq. (1). However, this would severely underestimate this DPS contribution, since soft gluon radiation must be taken into account in a more realistic simulation. Soft radiation destroys the p_T balance of the two jets in the dijet process, leading to the possibility of only one of the two final state partons to be identified as a jet, even though both satisfy the pseudo-rapidity requirements of Eq. (1). Since our tree-level calculation cannot properly take into account such effects, we conservatively select the higher-energy jet of the dijet process in the hemisphere opposite that of the jet from the $\gamma\gamma j$ event, and allow the third jet to be anywhere, completely ignoring it for the purposes of imposing further cuts.

A second DPS mode consists of two overlapping γj events. All final state particles must be observed above threshold in the detector. With full acceptance cuts this background is found to be

insignificant compared to the others, and will not be considered further. We do not consider DPS backgrounds from overlapping $\gamma\gamma$ and jj events since the double forward jet tagging requirements of Eq. (2) force the dijet invariant mass to be very large, effectively eliminating this background.

At the basic level of cuts (Eq. (1)), the backgrounds are overwhelming, the irreducible QCD component alone being up to two orders of magnitude larger than the signal in an $m_{\gamma\gamma} = m_H$ invariant mass bin of width 2 GeV. This is not surprising: the presence of $p_T = 20$ GeV jets is a common occurrence in hard scattering events at the LHC. The double forward jet tagging requirement of Eq. (2), with its concomitant large dijet invariant mass, reduces the signal by $\approx 50\%$ but decreases the total background by almost two orders of magnitude, below the level of the signal. We can reduce the backgrounds even further by employing harder p_T cuts on the jets and photons, and find that the following asymmetric p_T cuts bring the backgrounds down another factor of three, while accepting over 85% of the signal:

$$\begin{aligned} p_{T_{j1}} &\geq 40 \text{ GeV} , & p_{T_{j2}} &\geq 20 \text{ GeV} , \\ p_{T_{\gamma1}} &\geq 50 \text{ GeV} , & p_{T_{\gamma2}} &\geq 25 \text{ GeV} . \end{aligned} \tag{4}$$

For $m_H = 120$ GeV, the resulting signal cross section is 2.0 fb.

The effectiveness of these cuts stems from two differing characteristics of the signal and background. First, the generic $jj\gamma\gamma$ backgrounds are produced at small center of mass energies and are efficiently suppressed once we require a large invariant mass for the final state system, via the far forward rapidities of the two opposite-hemisphere tagging jets. Second, we expect the Higgs to be centrally produced, resulting in central photons, while background photons are primarily from bremsstrahlung off quarks. Since the jets are far forward, the photons will likewise tend to be at high average $|\eta|$. In addition, bremsstrahlung tends to be soft, and the harder p_T cuts on the photons quite efficiently reject bremsstrahlung events. We could require even higher p_{T_γ} cuts, making the backgrounds negligible, but this would come at the expense of a sizeable reduction in signal rate, leaving only a few events in 10 fb^{-1} of data.

Fig. 4 shows the results after the cuts of Eq. (4). This plot compares the total signal cross section, in fb, to the di-photon invariant mass distribution, $d\sigma/dm_{\gamma\gamma}$ in fb/GeV and thus indicates

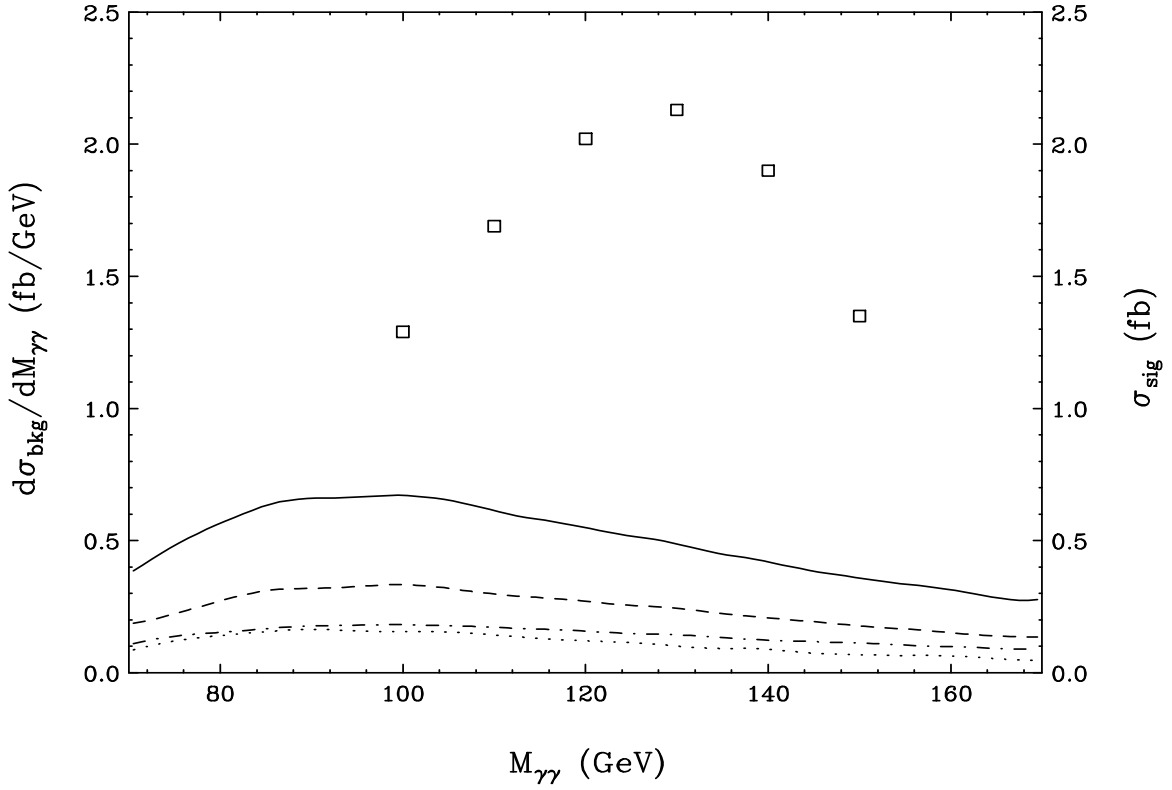


FIG. 4. Higgs boson signal cross section (in fb) and diphoton invariant mass distribution (in fb/GeV) for the backgrounds after the cuts of Eqs. (1,2,4). The squares are the Higgs signal for $m_H = 100, 110, 120, 130, 140, 150$ GeV. The solid line represents the sum of all backgrounds, with individual components from the irreducible QCD background (dashed line), the irreducible EW background (dot-dashed line), and for the double parton scattering (DPS) background (dotted line) shown below.

the relative size of signal and background for a mass resolution of $\Delta m_{\gamma\gamma} \approx \pm 0.5$ GeV. Actual resolutions are expected to be $\approx \pm 0.6 \cdots 1$ GeV for CMS and about ± 1.5 GeV for ATLAS [3]. For our cuts, with 10 fb^{-1} of data, we thus expect 13 to 21 $H \rightarrow \gamma\gamma$ events on a background of 14 to 7 events (for a resolution of ± 1 GeV). This corresponds to a 3.5 to 6.9 standard deviation signal. Thus, a Higgs boson discovery with a mere 10 fb^{-1} of data appears feasible in the $qq \rightarrow qqH \rightarrow jj\gamma\gamma$ channel. It should be noted, however, that this estimate does not consider detector efficiencies, nor a detailed analysis of resolution effects. Such a more detailed analysis is needed because more than 50% of the signal events have at least one jet with $|\eta| \leq 2.4$ (see

Fig 1), leading to charged particle tracks in the central detector. As a result, the position of the interaction vertex can be more accurately obtained, leading to improved photon invariant mass resolution. We leave detailed studies of detector performance to the experimental collaborations.

Limited detector efficiencies and resolutions can be compensated by exploiting another feature of the $qq \rightarrow qqH$ signal, namely the absence of color exchange between the two scattering quarks. As has been demonstrated for the analogous $qq \rightarrow qqZ$ process, with its very similar kinematics [15], t -channel color singlet exchange leads to soft jet emission mainly in the very forward and very backward regions, and even here mini-jet emission is substantially suppressed compared to QCD backgrounds. QCD processes are dominated by t -channel color octet exchange which results in minijet emission mainly in the central detector. These differences can be exploited in a central minijet veto [16] in double forward jet tagging events. From previous studies of weak boson scattering signals [15,17], we expect a veto on additional central jets of $p_{Tj} \gtrsim 20$ GeV to further reduce the QCD and DPS backgrounds by up to one order of magnitude, while affecting the signal at only the 10-20% level. These issues will be studied for the $H \rightarrow \gamma\gamma$ signal also [18]. With this additional background suppression we expect the discovery of the Higgs boson in the $qq \rightarrow qqH \rightarrow jj\gamma\gamma$ channel to be largely background free, and possible with an integrated luminosity of 10 fb^{-1} even when taking into account reduced detector efficiencies [3].

ACKNOWLEDGMENTS

This research was supported in part by the University of Wisconsin Research Committee with funds granted by the Wisconsin Alumni Research Foundation and in part by the U. S. Department of Energy under Contract No. DE-FG02-95ER40896.

REFERENCES

- [1] For a recent review, see e.g. J. L. Rosner, EFI-97-18, hep-ph/9704331 and references therein.
- [2] For a recent review, see e.g. S. Dawson, hep-ph/9703387 and references therein.
- [3] W. W. Armstrong *et al.*, Atlas Technical Proposal, report CERN/LHCC/94-43 (1994);
G. L. Bayatian *et al.*, CMS Technical Proposal, report CERN/LHCC/94-38 (1994).
- [4] W. J. Marciano and F. E. Paige, Phys. Rev. Lett. **66**, 2433 (1991); J. F. Gunion, Phys. Lett. **B261**, 510 (1991).
- [5] A. Stange, W. Marciano, and S. Willenbrock, Phys. Rev. **D50**, 4491 (1994), [hep-ph/9404247]; R. Kleiss, Z. Kunszt, W. J. Stirling, Phys. Lett. **B253**, 269 (1991); H. Baer, B. Bailey, J. F. Owens, Phys. Rev. **D47**, 2730 (1993).
- [6] V. Barger *et al.*, Phys. Rev. **D45**, 4128 (1992).
- [7] H.L. Lai *et al.*, Phys. Rev. **D55**, 1280 (1997), [hep-ph/9606399].
- [8] R. N. Cahn *et al.*, Phys. Rev. **D35**, 1626 (1987); V. Barger, T. Han, and R. J. N. Phillips, Phys. Rev. **D37**, 2005 (1988); R. Kleiss and W. J. Stirling, Phys. Lett. **200B**, 193 (1988); D. Froideveaux, in *Proceedings of the ECFA Large Hadron Collider Workshop*, Aachen, Germany, 1990, edited by G. Jarlskog and D. Rein (CERN report 90-10, Geneva, Switzerland, 1990), Vol II, p. 444; M. H. Seymour, *ibid*, p. 557; U. Baur and E. W. N. Glover, Nucl. Phys. **B347**, 12 (1990); Phys. Lett. **B252**, 683 (1990).
- [9] V. Barger *et al.*, Phys. Rev. **D42**, 3052 (1990); V. Barger *et al.*, Phys. Rev. **D44**, 1426 (1991); V. Barger *et al.*, Phys. Rev. **D44**, 2701 (1991); erratum Phys. Rev. **D48**, 5444 (1993); Phys. Rev. **D48**, 5433 (1993); V. Barger *et al.*, Phys. Rev. **D46**, 2028 (1992).
- [10] D. Dicus, J. F. Gunion, and R. Vega, Phys. Lett. **B258**, 475 (1991); D. Dicus, J. F. Gunion, L. H. Orr, and R. Vega, Nucl. Phys. **B377**, 31 (1991).
- [11] V. Barger *et al.*, Phys. Rev. **D41**, 2782 (1990).

- [12] T. Stelzer and W. F. Long, *Comp. Phys. Comm.* **81**, 357 (1994), [hep-ph/9401258].
- [13] F. Halzen, P. Hoyer, and W. J. Stirling, *Phys. Lett.* **188B**, 375, 1987; M. Drees and T. Han, *Phys. Rev. Lett.* **77**, 4142 (1996), [hep-ph/9605430].
- [14] S. Behrends and J. Lamoureux, FERMILAB-CONF-97-204-E (1997).
- [15] D. Rainwater, R. Szalapski, and D. Zeppenfeld, *Phys. Rev.* **D54**, 6680 (1996), [hep-ph/9605444].
- [16] V. Barger, R. J. N. Phillips, and D. Zeppenfeld, *Phys. Lett.* **B346**, 106 (1995), [hep-ph/9412276].
- [17] K. Iordanidis and D. Zeppenfeld, preprint MADPH-97-1017 (1997), [hep-ph/9709506];
- [18] D. Rainwater and D. Zeppenfeld, in preparation.